

## Long-Term Variability of Electron Radiation Dose in Geosynchronous Orbit

30 November 1994

Prepared by

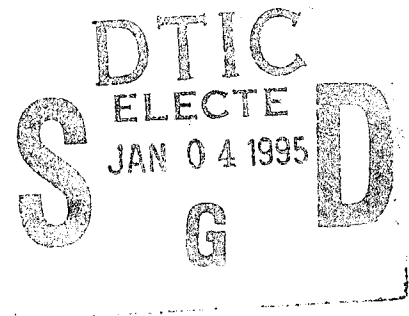
H. C. KOONS, D. J. GORNEY, and J. B. BLAKE  
Space and Environment Technology Center  
Technology Operations

Prepared for

SPACE AND MISSILE SYSTEMS CENTER  
AIR FORCE MATERIEL COMMAND  
2430 E. El Segundo Boulevard  
Los Angeles Air Force Base, CA 90245

Engineering and Technology Group

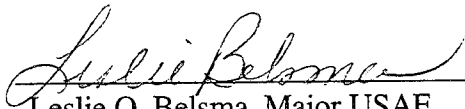
19941229 003



This report was submitted by The Aerospace Corporation, El Segundo, CA 90245-4691, under Contract No. F04701-93-C-0094 with the Space and Missile Systems Center, 2430 E. El Segundo Blvd., Los Angeles Air Force Base, CA 90245. It was reviewed and approved for The Aerospace Corporation by A. B. Christensen, Principal Director, Space and Environment Technology Center. Maj. Leslie Belsma was the project officer.

This report has been reviewed by the Public Affairs Office (PAS) and is releasable to the National Technical Information Service (NTIS). At NTIS, it will be available to the general public, including foreign nationals.

This technical report has been reviewed and is approved for publication. Publication of this report does not constitute Air Force approval of the report's findings or conclusions. It is published only for the exchange and stimulation of ideas.

  
\_\_\_\_\_  
Leslie O. Belsma, Major USAF  
SMC/IMO

REPORT DOCUMENTATION PAGE			Form Approved OMB No. 0704-0188	
Public reporting burden for this collection of information is estimated to average 1 hour per response, including the time for reviewing instructions, searching existing data sources, gathering and maintaining the data needed, and completing and reviewing the collection of information. Send comments regarding this burden estimate or any other aspect of this collection of information, including suggestions for reducing this burden to Washington Headquarters Services, Directorate for Information Operations and Reports, 1215 Jefferson Davis Highway, Suite 1204, Arlington, VA 22202-4302, and to the Office of Management and Budget, Paperwork Reduction Project (0704-0188), Washington, DC 20503.				
1. AGENCY USE ONLY (Leave blank)		2. REPORT DATE 30 November 1994		3. REPORT TYPE AND DATES COVERED
4. TITLE AND SUBTITLE Long-Term Variability of Electron Radiation Dose in Geosynchronous Orbit			5. FUNDING NUMBERS  F04701-93-C-0094	
6. AUTHOR(S)  Authors here				
7. PERFORMING ORGANIZATION NAME(S) AND ADDRESS(ES) The Aerospace Corporation Technology Operations El Segundo, CA 90245-4691			8. PERFORMING ORGANIZATION REPORT NUMBER  TR-93(3940)-13	
9. SPONSORING/MONITORING AGENCY NAME(S) AND ADDRESS(ES) Space and Missile Systems Center Air Force Materiel Command 2430 E. El Segundo Boulevard Los Angeles Air Force Base, CA 90245			10. SPONSORING/MONITORING AGENCY REPORT NUMBER  SMC-TR-95-49	
11. SUPPLEMENTARY NOTES				
12a. DISTRIBUTION/AVAILABILITY STATEMENT  Approved for public release; distribution unlimited			12b. DISTRIBUTION CODE	
13. ABSTRACT (Maximum 200 words)  A neural network that was developed to model the temporal variations of relativistic (>3 MeV) electrons at geosynchronous orbit has been used to estimate the long-term variability of the radiation dose to geosynchronous spacecraft. The input to the neural network consists of 10 consecutive days of the daily sum of the planetary magnetic index $\Sigma Kp$ . The output is an estimate of the daily-averaged electron flux for the tenth day. The model was used to compute the daily-averaged electron flux for energies >3 MeV for each day from January 1933 through December 1988. Assuming that the average energy spectrum is independent of time, the annual radiation dose of electrons >300 keV is obtained by scaling the model output to 300 keV and summing the daily-averaged flux for each year. The annual dose is found to vary from 0.25 3.4 times its average value. The dose is found to correlate only weakly with the annual mean sunspot number. The results are also applicable to studies of the effect on the middle atmosphere of the long-term variability of the precipitation of these electrons into the atmosphere.				
14. SUBJECT TERMS  Radiation dose, Geosynchronous orbit, Neural network, Electron precipitation			15. NUMBER OF PAGES 5	
			16. PRICE CODE	
17. SECURITY CLASSIFICATION OF REPORT UNCLASSIFIED	18. SECURITY CLASSIFICATION OF THIS PAGE UNCLASSIFIED	19. SECURITY CLASSIFICATION OF ABSTRACT UNCLASSIFIED	20. LIMITATION OF ABSTRACT	

## Contents

Nomenclature .....	1
Introduction .....	1
Neural Network Model .....	2
Radiation Dose Results.....	2
Comparison with Measurements.....	4
Discussion .....	4
Accuracy of Radiation Belt Models.....	4
Future Work .....	4
Acknowledgments .....	4
References .....	4

## Figures

1. Composite electron spectra from 10 keV to 10 MeV.....	2
2. Power-law fit to the spectra in Fig. 1 over the energy range from 240 keV to 4 MeV.....	3
3. Annual fluences of electrons with energies >300 keV at geosynchronous orbit as a function of time .....	3
4. Ratio of the annual fluence of electrons with energies >300 keV to their average annual fluence for the years of 1933-1988.....	3
5. Probability distribution function of the annual fluence of electrons with energies >300 keV at geosynchronous orbit.....	4
6. Scatter plot of the annual fluence of electrons with energies >300 keV vs mean annual sunspot number.....	4
7. Comparison of the annual fluence of relativistic electrons with energies >3 MeV.....	4

r	
4	<input checked="" type="checkbox"/>
d	<input type="checkbox"/>
By .....	
Distribution / .....	
Availability Codes	
Dist	Avail and/or Special
A-1	

### Nomenclature

$A$	= scaling constant
$E$	= electron energy, keV
$E_L$	= low energy limit for integration, keV
$E_0$	= electron e-folding energy, keV
$E_1$	= electron energy, 300 keV
$E_2$	= electron energy, 3000 keV
$F_1$	= average daily electron fluence above energy $E_1$
$J$	= electron flux, $\text{cm}^2/\text{s-sr}$
$J_1$	= integral electron flux above energy $E_1$ , $\text{cm}^2/\text{s-sr}$
$J_2$	= integral electron flux above energy $E_2$ , $\text{cm}^2/\text{s-sr}$
$K_p$	= planetary magnetic index
$k$	= power-law exponent
$R$	= ratio of the integral electron flux above $E_1$ to that above $E_2$
$W$	= weight matrix between neurons in two layers of the neural network
$W_{ij}$	= connection strength between neuron $i$ and neuron $j$
$\Delta t$	= time interval, seconds in one day = 86,400 s
$\Sigma K_p$	= daily sum of the planetary magnetic index, $K_p$
$\Omega$	= solid angle, sr

### Introduction

THE long-term variability of relativistic electrons in the Earth's radiation belts determines the variability of the radiation dose to spacecraft components and contributes to the variability of electron precipitation into the middle atmosphere. The variability of the dose influences spacecraft design, and the variability of the electron precipitation may have climatological consequences.

Energetic electrons in the Earth's radiation belts pose a significant hazard to electronic components on spacecraft.<sup>1</sup> The total radiation dose to a lightly shielded component can be orders of magnitude larger than typical susceptibility levels. This

necessitates the use of additional shielding material which adds significantly to the total weight of the vehicle.

Models of the electron environment are used to calculate the total radiation dose for specific orbits. The results of such computations, together with susceptibility data, are used to specify the minimum shielding required for spacecraft electronics. A variety of models have been developed for this purpose by the National Space Science Data Center. The electron model in current use is AE-8.<sup>2</sup> This model is essentially static and is thus only valid for conditions similar to those present when the measurements were originally made. There is some provision for variability. AE-8 actually consists of two models—one for solar maximum and one for solar minimum. The solar maximum model predicts higher fluxes and thus is the more severe.

Measurements of highly relativistic electrons performed from 1979 to 1984 by the Los Alamos spectrometer for energetic electrons (SEE) spectrometers on geosynchronous spacecraft showed only sporadic increases in the electrons from 1979 to 1981 around solar maximum but frequent increases during the declining phase of the solar cycle from 1982 to 1984.<sup>3</sup> The models are thus contrary to those measurements. A serious shortcoming in the effort to develop long-term models is the lack of a consistent long-term set of measurements.

Thorne<sup>4,5</sup> has suggested that the precipitation of energetic magnetospheric electrons might be a mechanism by which solar-magnetospheric processes could significantly affect the middle atmosphere and perhaps have climatological effects. This idea was extended by Baker et al.<sup>6</sup> using long-term measurements of energetic magnetospheric electrons and studied further using measurements of atmospheric optical emissions in concert with electron measurements by Callis et al.<sup>7,8</sup> Because the magnetospheric population of energetic electrons varies in an irregular and poorly understood way with solar activity and the solar cycle, it is crucial to have a reliable, long term database describing these electrons for correlation with atmospheric studies.

We have developed a neural network to model the temporal variations of the relativistic electron flux at geosynchronous orbit.<sup>9</sup> The results reported here from the neural network model provide the first estimate of the long-term variability of these energetic magnetospheric electrons.

The model takes as inputs 10 consecutive values of the daily-summed planetary magnetic index  $\Sigma K_p$ . The output is an estimate of the daily-averaged electron flux for energies  $>3$

Received May 1, 1992; revision received July 12, 1993; accepted for publication July 23, 1993. Copyright © 1993 by the American Institute of Aeronautics and Astronautics, Inc. All rights reserved.

\* Senior Scientist, Space and Environment Technology Center, P.O. Box 92957, Member AIAA.

† Director, Atmospheric and Ionospheric Sciences Department, Space and Environment Technology Center, P.O. Box 92957, Member AIAA.

‡ Director, Space Particles and Fields Department, Space and Environment Technology Center, P.O. Box 92957.

MeV for the tenth day. This model provides an accurate simulation and forecasting tool for the geosynchronous electron environment. In particular, the model can be used to infer electron fluxes for time periods during which direct measurements are not available.

$Kp$  indices from 1932 to date derived at the Geophysical Institute, Göttingen University, are available from the National Oceanic and Atmospheric Administration (NOAA), National Geophysical Data Center.<sup>10</sup> They provide over 50 years of input for the neural network model. We have run the model using  $\Sigma Kp$  calculated from these  $Kp$  indices to estimate the long-term temporal variability of the relativistic electron flux at geosynchronous orbit. We have also estimated the annual radiation dose due to electrons to a lightly shielded electronic component at synchronous orbit over this same time period. The results are described here.

### Neural Network Model

The neural network used for this application has been described by Koons and Gorney.<sup>9</sup> We will only repeat here the salient features that will help the reader to understand this application. The neural network consists of three layers of neurons. The 10 neurons that comprise the first layer are connected to the input, consisting of the values of  $\Sigma Kp$  for 10 consecutive days. Day 0 is defined to be the day for which the electron flux is calculated. The second layer of neurons, often referred to as the hidden layer, consists of 6 neurons. It is common to construct neural networks such that the number of hidden neurons is half the sum of the number of inputs and outputs. A single neuron is connected to the output which represents the logarithm of the average flux of electrons for day 0.

Connections only exist between any single neuron and the neurons in the previous layer of the network. Neurons within a given layer do not connect to each other and do not receive inputs from subsequent layers. For example, neurons in layer 1 send outputs to layer 2, and neurons in layer 2 take inputs from layer 1 and send outputs to layer 3. The connection strengths between any two layers constitute the elements of a real-valued matrix ( $W$ ). The elemental values  $W_{ij}$  represent the connection strength or weight between neuron  $i$  (in one layer) to neuron  $j$  (in the next higher layer). The weight matrices are modified by training using actual data, and these matrices ultimately contain all of the information relating the input ( $\Sigma Kp$ ) to the output (the logarithm of the electron flux).

The network was trained and tested using electron data collected by a spectrometer for energetic electrons instrument. The SEE sensor was designed and built by the Los Alamos National Laboratory. For a description of the instrument see Baker et al.<sup>3</sup> This design has flown aboard a number of geostationary satellites. An edited data set covering the period from April 19, 1982 to June 4, 1988 from one spacecraft, 1982-019, was provided for our use. The data set consists of daily average count rates with the galactic cosmic-ray background removed.

The network was trained using count rates from the high-energy ( $>3$  MeV) electron channel. The results were converted to flux using a geometric factor of  $0.08 \text{ cm}^2\text{-sr}$  and an efficiency of 0.3 for the 3-MeV channel. The training data set consisted of 62 days of data from July 1, 1984, to August 31, 1984. The training interval was selected on the basis of data continuity and the occurrence of several large discrete flux enhancements within the chosen interval. The probability distribution function for the flux for the training period is qualitatively similar to the distribution function for the observations for the entire period from 1982 to 1988 as shown in Fig. 6 in Koons and Gorney.<sup>9</sup> However, the training period has some excess values of high flux consistent with its selection as a period of significant flux enhancements. To obtain convergence in the neural network, the training criteria was set at 10% of the complete range of output, corresponding to  $\sim 0.5$  for the logarithm of the flux or, equivalently, about a factor of three. Training required 2652

passes through the 62 patterns in the training set. The weight matrices and threshold neuron values for the trained network are given in Koons and Gorney.<sup>9</sup>

The model was tested by comparing the model outputs with measured fluxes over the entire six-year period from April 19, 1982 to June 4, 1988. For the entire data set the rms logarithmic error of the neural network is 0.76 and the average logarithmic error is 0.58.

### Radiation Dose Results

The annual radiation dose due to electrons to a lightly shielded electronic component at geosynchronous orbit is taken to be the total annual dose from electrons with energies greater than 300 keV. We can use the results from the neural network model to estimate this number under the assumption that the shape of the average energy spectrum above 300 keV is independent of time. To obtain the annual dose, we first estimate the dose for each day for energies  $>3$  MeV from the neural network model. We then scale this dose to energies  $>300$  keV and finally sum over the days in the year. We have used electron spectral data from the literature to determine the proper scaling.

Figure 1 shows observed average electron spectra from 10 keV to 10 MeV. The energies between the dotted vertical lines in the figure are the energies of interest to this paper. The figure is a composite of data from the rapid scan particle detector (RSPD) on the SCATHA satellite,<sup>11</sup> the high energy particle spectrometer (HEPS) on SCATHA,<sup>11</sup> the charged particle analyzer (CPA) on satellite 1979-053,<sup>12</sup> and the spectrometer for energetic electrons on 1979-053.<sup>3</sup> The RSPD data were obtained from Fig. 10 of Ref. 11. They are the differential number flux as a function of energy for perpendicular electrons averaged over all  $Kp$  and  $L$  shells for 00-01-h LT (squares) and 12-13-h LT (triangles). The data are comprised of measurements from 118 days during the period from Feb. 28, 1979 to June 14, 1980. The HEPS data were obtained from Table 38 and Fig. 58 in Ref. 13. It consists of the average energy spectrum at  $L = 6.75$  from 74 days between Feb. 11, 1979 and Feb. 16, 1980. Although the day-to-day variation is very large, Mullen and Gussenhoven<sup>13</sup> found the correlation coefficients for a power-law fit to the average energy spectra exceeded 0.99 for the energy channels at 0.83, 1.2225, and 2.011 MeV. The CPA and SEE data were obtained from Fig. 7 in Ref. 3. The three curves are the energy spectra for June 10, 12, and 15, 1980. These days bracket a magnetic storm with  $Kp$  reaching 6+ on June 11, 1980. The low fluxes (stars) were observed on the day before the storm. The intermediate fluxes (diamonds) were observed on the day following the storm. The high fluxes (hexagons) were observed four days after the storm. The general

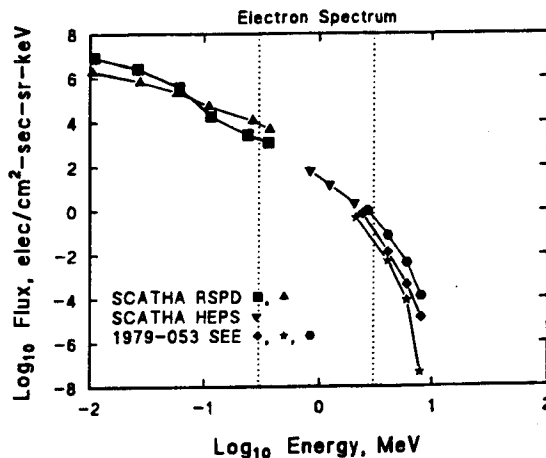


Fig. 1 Composite electron spectra from 10 keV to 10 MeV.

consistency among the spectra in Fig. 1 suggests that a fit to the data in the 0.3–3 MeV range will produce a reasonable spectral shape for the average electron spectrum.

Baker et al.<sup>6</sup> fit the high-energy component (>1 MeV) of the CPA and SEE data to an exponential spectrum of the form

$$\frac{dJ}{dE} = \left(\frac{dJ}{dE}\right)_0 \exp\left(\frac{-E}{E_0}\right) \left(\frac{\text{cm}^2}{\text{s-sr-keV}}\right) \quad (1)$$

and obtained an  $e$ -folding energy  $E_0$  of 0.587 MeV. Mullen and Gussenhoven<sup>13</sup> fit the HEPS data to a power law of the form

$$\frac{dJ}{dE} = AE^k \left(\frac{\text{cm}^2}{\text{s-sr-keV}}\right) \quad (2)$$

and obtained a value for the exponent of  $k = -3.88$ .

We have fit the data from 240 keV to 4.0 MeV with both an exponential and a power-law spectral shape. The better fit, shown in Fig. 2, is achieved with the power law with  $k = -4.5$ . Again the energies between the dotted vertical lines in the figure are the energies of interest to this paper. The correlation coefficient  $r$  is 0.975. For the exponential fit  $E_0 = 0.311$  MeV and  $r = 0.959$ . This value for  $E_0$  is considerably smaller than the value of 0.578 MeV obtained by Baker et al.<sup>6</sup> for the fit to the higher energy portion of the spectrum.

The integral flux above energy  $E_L$  is given by the double integral over solid angle and energy

$$J = \int_0^{4\pi} \int_{E_L}^{\infty} AE^k dE d\Omega \quad (3)$$

$$J = -4\pi AE_L^{k+1} / (k+1) \quad (4)$$

The ratio  $R$  of the integral flux above energy  $E_1$  to the integral flux above energy  $E_2$  is then given by

$$R = J_1/J_2 = (E_1/E_2)^{k+1} \quad (5)$$

If  $E_1$  is 300 keV and  $E_2$  is 3 MeV, then the ratio for  $k = -4.5$  is 3160. If the instantaneous integral flux above 3 MeV  $J_2$  is known, then the average daily fluence  $F_1 > 300$  keV is given by

$$F_1 = RJ_2 \Delta\Omega \Delta t \quad (6)$$

where  $J_2$  is the instantaneous integral flux averaged over a day

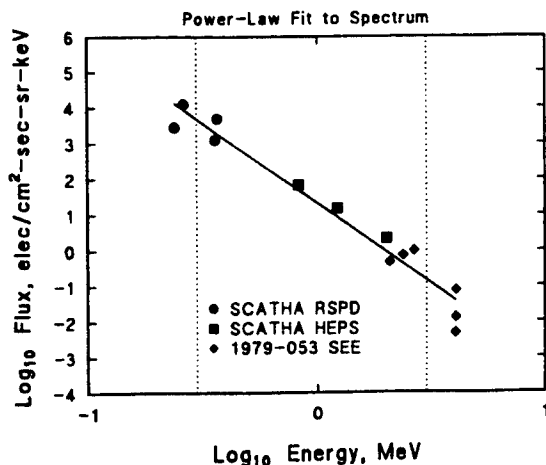


Fig. 2 Power-law fit to the spectra in Fig. 1 over the energy range from 240 keV to 4 MeV.

for electrons with energies greater than 3 MeV. For  $\Delta\Omega = 4\pi$  and  $\Delta t = 86400$  s,  $F_1 = 3.43 \times 10^9 J_2$ .

This technique was used to calculate the average daily fluence for each day from January 1, 1933 through December 31, 1988. The annual fluences were then calculated by summing the daily fluences over all of the days in each year. The resulting annual fluences are shown as a function of time as the solid curve in Fig. 3. Figure 4 shows the ratio of the annual fluence to its average value for the entire period from 1933 through 1988. The values range from 0.25 to 3.4 times the average value which is  $9.16 \times 10^{13} \text{ cm}^{-2}$ . The probability distribution function for the annual fluence is shown in Fig. 5. The total width of the distribution is about an order of magnitude, spanning the range from  $3.5 \times 10^{13}$  to  $3.5 \times 10^{14} \text{ cm}^{-2}$ .

The early spacecraft measurements suggested that the annual electron fluences were related to the sunspot cycle.<sup>14,15</sup> The annual mean sunspot numbers for the years from 1933 to 1988 are shown as the dotted curve in Fig. 3. A comparison of the data sets plotted in Fig. 3 shows that the temporal behavior of the electron fluences only weakly resembles that of the sunspot cycle. A scatter plot of the  $\log_{10}$  of the annual electron fluence vs the mean annual sunspot number is shown in Fig. 6. The solid line shows the best linear fit to the data. It is given by

$$\log_{10} \text{ fluence} = 13.82 + 0.002 \times \text{SSN} \quad (7)$$

where SSN is the annual mean sunspot number. The correlation

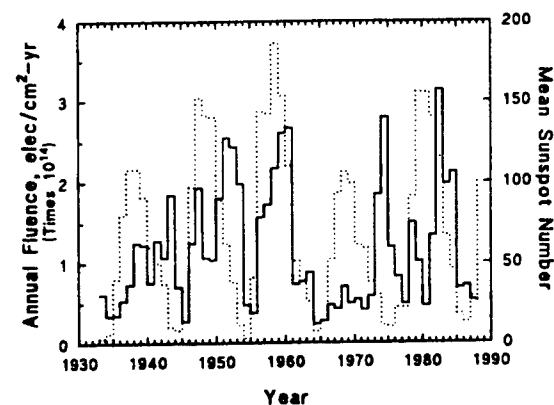


Fig. 3 Annual fluence of electrons with energies >300 keV at geosynchronous orbit as a function of time calculated using the neural network model, solid curve; mean annual sunspot number as a function of time, dotted curve.

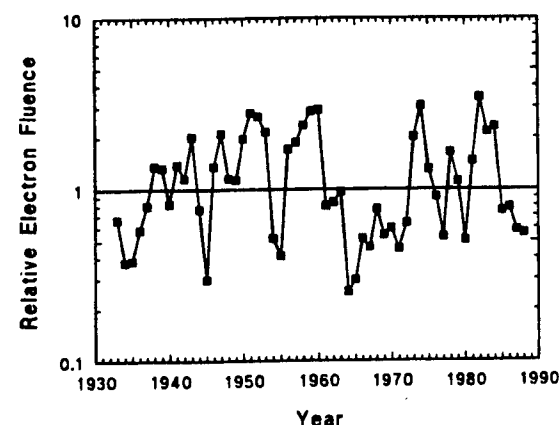


Fig. 4 Ratio of the annual fluence of electrons with energies >300 keV to their average annual fluence for the years of 1933–1988.

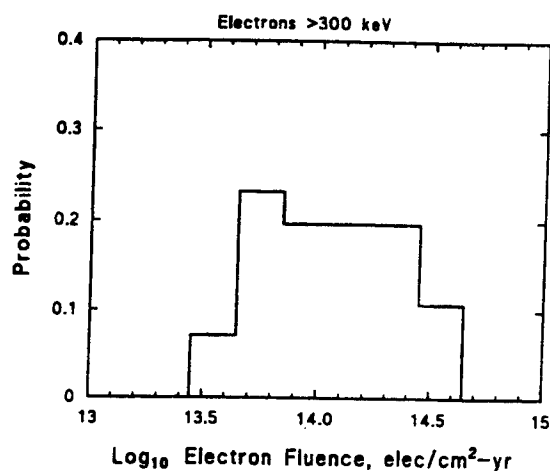


Fig. 5 Probability distribution function of the annual fluence of electrons with energies  $>300$  keV at geosynchronous orbit.

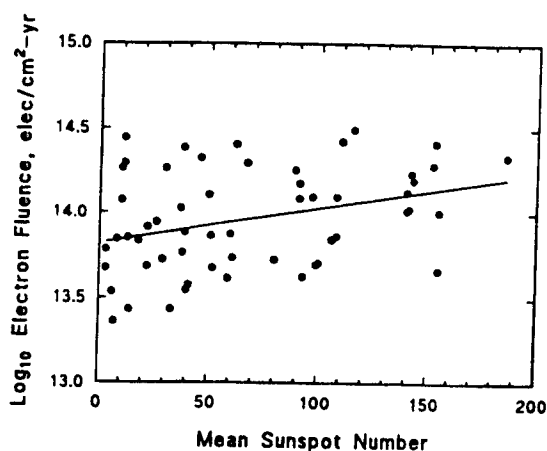


Fig. 6 Scatter plot of the annual fluence of electrons with energies  $>300$  keV vs mean annual sunspot number.

coefficient between the  $\log_{10}$  flux and the mean sunspot number is only 0.35.

Although there is a clear trend toward higher annual fluxes with increasing sunspot number the variation is very wide, and one of the highest predicted fluences occurs at one of the lowest sunspot numbers.

#### Comparison with Measurements

The results from the neural network model agree qualitatively with the measurements of relativistic electrons performed from 1979 to 1984 by the Los Alamos SEE spectrometers on geosynchronous spacecraft. These measurements showed only sporadic increases in the electrons from 1979 to 1981 around solar maximum but frequent increases during the declining phase of the solar cycle from 1982 to 1984.<sup>1</sup> The neural network model produces  $\log_{10}$  electron fluences of 14.01, 13.63, and 14.09 for 1979–1981 and 14.47, 14.27, and 14.29 for 1982–1984. Thus the earlier three years were all near the low end of the probability distribution function shown in Fig. 5 whereas the latter three years were near the high end.

Figure 7 shows a comparison of the estimate of the annual fluence from the neural network model with the observed average annual fluence determined from the observations for the years 1983–1987. The unscaled data at energies  $>3$  MeV were

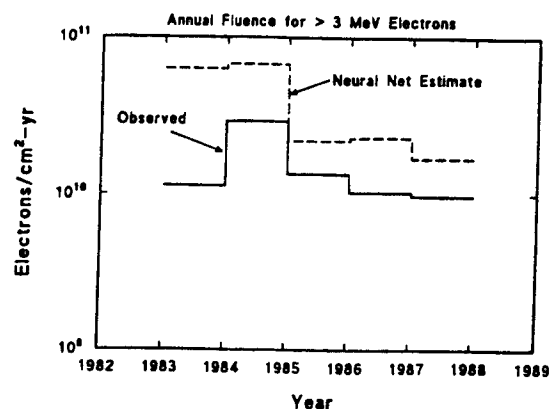


Fig. 7 Comparison of the annual fluence of relativistic electrons with energies  $>3$  MeV as estimated by using the neural network model (dashed curve); and as observed, solid curve.

used for the comparison in Fig. 7. The neural network estimate is systematically high by a factor of 2.4. The correlation coefficient between the estimated and the observed fluence is 0.64. This relatively low correlation is primarily caused by a large discrepancy (a factor of 5.6) in 1983. Excluding that year the correlation coefficient is 0.97.

#### Discussion

##### Accuracy of Radiation Belt Models

A curious feature of the annual fluences predicted by the model is the long period of low fluences shown in Fig. 3 in 1961–1972. Unfortunately, most of the observations that were used to produce the electron models by NSSDC were made by spacecraft during this time period. The low fluence values shown in Fig. 3 during the 1960s suggest that the electron models might be low by about a factor of two.

##### Future Work

The main limitation of the present work is the assumption that the shape of the differential energy spectrum of the relativistic electrons is independent of time and on average is given by a power law with  $k = -4.5$  in the range from 300 keV to 3 MeV. Further work is required to determine the validity of this assumption. The flux is observed to be highly variable, and the spectrum tends to harden as the flux increases. This is apparent in the data shown in Fig. 1 above 2 MeV. It must still be determined if there is a long-term secular variation to the shape of the average energy spectrum in the energy range discussed in this paper.

#### Acknowledgments

This work was supported by the Space and Missile Systems Center of the U.S. Air Force under Contract F04701-88-C-0089. The authors thank R. Klebesadel and D. Baker for the electron data from spacecraft 1982-019 that were used to generate and test the neural network model. We wish to thank M. Schulz for useful discussions on relativistic electron intensities in the outer radiation belt. The values of  $Kp$  used in this study were obtained from NOAA's Environmental Data and Information Service, National Geophysical Data Center.

#### References

- <sup>1</sup>Gorney, D. J., Blake, J. B., Koons, H. C., Schulz, M., Vampola, A., and Walterscheid, R. L., "The Space Environment and Survivability," *Space Mission Analysis and Design*, edited by J. R. Wertz and W. J. Larson, Kluwer Academic, Boston, MA, 1991, pp. 185–190.
- <sup>2</sup>Bilitza, D., Sawyer, D. M., and King, J. H., "Trapped Particle Models at NSSDC/WDC-A-R&S," *NASA/SDIO Space Environmental*



*Effects on Materials Workshop*, NASA Conference Pub. 3035, Pt. 2, Hampton, VA, June 1988, edited by B. A. Stein and L. A. Teichman, 1989, pp. 569-572.

<sup>3</sup>Baker, D. N., Blake, J. B., Klebesadel, R. W., and Higbie, P. R., "Highly Relativistic Electrons in the Earth's Outer Magnetosphere, I. Lifetimes and Temporal History 1979-1984," *Journal of Geophysical Research*, Vol. 91, April 1986, pp. 4265-4276.

<sup>4</sup>Thorne, R. M., "Influence of Relativistic Electron Precipitation on the Lower Ionosphere and Stratosphere," *Dynamical and Chemical Coupling Between the Neutral And Ionized Atmosphere*, edited by B. Grandal and J. A. Holter, D. Reidel, Boston, MA, 1977, pp. 161-168.

<sup>5</sup>Thorne, R. M., "The Importance of Energetic Particle Precipitation on the Chemical Composition of the Middle Atmosphere," *Pure and Applied Geophysics*, Vol. 118, Jan. 1980, pp. 128-151.

<sup>6</sup>Baker, D. N., Blake, J. B., Gorney, D. J., Higbie, P. R., Klebesadel, R. W., and King, J. H., "Highly Relativistic Magnetospheric Electrons: A Role in Coupling to the Middle Atmosphere?," *Geophysical Research Letters*, Vol. 14, Oct. 1987, pp. 1027-1030.

<sup>7</sup>Callis, L. B., Boughner, R. E., Natarajan, M., Lambeth, J. D., Baker, D. N., and Blake, J. B., "Ozone Depletion in the High Latitude Lower Stratosphere: 1979-1990," *Journal of Geophysical Research*, Vol. 96, Feb. 1991, pp. 2921-2937.

<sup>8</sup>Callis, L. B., Baker, D. N., Blake, J. B., Lambeth, J. D., Boughner, R. E., Natarajan, M., Klebesadel, R. W., and Gorney, D. J., "Precipitating Relativistic Electrons: Their Long-Term Effect on Stratospheric Odd Nitrogen Levels," *Journal of Geophysical Research*, Vol. 96, Feb. 1991, pp. 2939-2976.

<sup>9</sup>Koons, H. C., and Gorney, D. J., "A Neural Network Model of the Relativistic Electron Flux at Geosynchronous Orbit," *Journal of Geophysical Research*, Vol. 96, April 1991, pp. 5549-5556.

<sup>10</sup>Menvielle, M., and A. Berthelier, "The K-Derived Planetary Indices: Description and Availability," *Reviews of Geophysics*, Vol. 29, Aug. 1991, pp. 415-432.

<sup>11</sup>Stevens, J. R., and Vampola, A. L., "Description of the Space Test Program P78-2 Spacecraft and Payloads," Air Force Systems Command, Space and Missile Systems Organization, SAMSO TR-78-24, Los Angeles, CA, Oct. 1978.

<sup>12</sup>Baker, D. N., Belian, R. D., Higbie, P. R., and Hones, E. W., Jr., "High-Energy Magnetospheric Protons and Their Dependence on Geomagnetic and Interplanetary Conditions," *Journal of Geophysical Research*, Vol. 84, Dec. 1979, pp. 7138-7154.

<sup>13</sup>Mullen, E. G., and Gussenhoven, M. S., "SCATHA Environmental Atlas," Air Force Geophysics Lab., AFGL-TR-83-0002, Hanscom AFB, MA, Jan. 1983.

<sup>14</sup>Teague, M. J., and Vette, J. I., "A Model of the Trapped Electron Population for Solar Minimum," National Space Science Data Center, NSSDC/WDC-A-R&S 74-03, Goddard Space Flight Center, Greenbelt, MD, April 1974.

<sup>15</sup>Teague, M. J., Chan, K. W., and Vette, J. I., "AE6: A Model Environment for Trapped Electrons for Solar Maximum," National Space Science Data Center, NSSDC/WDC-A-R&S 76-04, Goddard Space Flight Center, Greenbelt, MD, May 1976.

## TECHNOLOGY OPERATIONS

The Aerospace Corporation functions as an "architect-engineer" for national security programs, specializing in advanced military space systems. The Corporation's Technology Operations supports the effective and timely development and operation of national security systems through scientific research and the application of advanced technology. Vital to the success of the Corporation is the technical staff's wide-ranging expertise and its ability to stay abreast of new technological developments and program support issues associated with rapidly evolving space systems. Contributing capabilities are provided by these individual Technology Centers:

**Electronics Technology Center:** Microelectronics, solid-state device physics, VLSI reliability, compound semiconductors, radiation hardening, data storage technologies, infrared detector devices and testing; electro-optics, quantum electronics, solid-state lasers, optical propagation and communications; cw and pulsed chemical laser development, optical resonators, beam control, atmospheric propagation, and laser effects and countermeasures; atomic frequency standards, applied laser spectroscopy, laser chemistry, laser optoelectronics, phase conjugation and coherent imaging, solar cell physics, battery electrochemistry, battery testing and evaluation.

**Mechanics and Materials Technology Center:** Evaluation and characterization of new materials: metals, alloys, ceramics, polymers and their composites, and new forms of carbon; development and analysis of thin films and deposition techniques; nondestructive evaluation, component failure analysis and reliability; fracture mechanics and stress corrosion; development and evaluation of hardened components; analysis and evaluation of materials at cryogenic and elevated temperatures; launch vehicle and reentry fluid mechanics, heat transfer and flight dynamics; chemical and electric propulsion; spacecraft structural mechanics, spacecraft survivability and vulnerability assessment; contamination, thermal and structural control; high temperature thermomechanics, gas kinetics and radiation; lubrication and surface phenomena.

**Space and Environment Technology Center:** Magnetospheric, auroral and cosmic ray physics, wave-particle interactions, magnetospheric plasma waves; atmospheric and ionospheric physics, density and composition of the upper atmosphere, remote sensing using atmospheric radiation; solar physics, infrared astronomy, infrared signature analysis; effects of solar activity, magnetic storms and nuclear explosions on the earth's atmosphere, ionosphere and magnetosphere; effects of electromagnetic and particulate radiations on space systems; space instrumentation; propellant chemistry, chemical dynamics, environmental chemistry, trace detection; atmospheric chemical reactions, atmospheric optics, light scattering, state-specific chemical reactions and radiative signatures of missile plumes, and sensor out-of-field-of-view rejection.